

## Density Functional Study of Lithium Hexamethyldisilazide (LiHMDS) Complexes: Effects of Solvation and Aggregation

Svetlana Popenova,<sup>†,§</sup> Robert C. Mawhinney,<sup>†,‡</sup> and Georg Schreckenbach<sup>\*,‡</sup>

Department of Chemistry and Biochemistry, Concordia University, Montreal QC, Canada H3G 1M8, and Department of Chemistry, University of Manitoba, Winnipeg MB, Canada, R3T 2N2

Received August 23, 2006

The title compound, lithium hexamethyldisilazide (LiHMDS), has been studied using modern quantum-chemical methods in the form of the B3LYP approach. Monomers, dimers, trimers, and tetramers, microsolvated with up to four THF molecules have been considered. The choice of model complex is seen to be important—for instance, the simpler water molecule is shown to be an inappropriate substitute for the THF solvent. Calculated lithium NMR shieldings are reported, but by themselves, they seem to be insufficient for unequivocal assignments of the different species. The energetics of aggregation and solvation have been studied. Temperature effects are seen to be important, and the degrees of solvation and aggregation are higher at 0 K than at 298 K. The highest degree of THF solvation for the monomer and dimer is found to be three (0 K) and two (298 K), respectively. The highest possible degree of aggregation for unsolvated LiHMDS is four. However, in nonpolar solvents, formation of the LiHMDS dimer from the trimer is thermodynamically preferred. The pathway is likely to involve an intermediate tetramer. In THF solution, di-solvated monomers and dimers are the most likely species.

### Introduction

Lithium amide complexes are widely used in organic and organometallic synthesis as nucleophilic or basic reagents. Moreover, they are of interest as potential precursors for metal–organic vapor deposition, aiming at advanced battery materials, for instance.<sup>1,2</sup>

The general formula for these complexes is  $(R'RNLi \cdot xL)_n$ , where L is the (usually polar) solvent, x is the degree of solvation, R and R' are organic ligands (possibly binding through a heteroatom, for example, P, S, or Se), and n is the degree of aggregation. In solution, these complexes exist in monomeric ( $n = 1$ ), dimeric ( $n = 2$ ), and higher oligomeric forms. Moreover, most of them are capable of forming solvent complexes (i.e.,  $x > 0$ ). There is a great variety in the coordination chemistry of lithium, not only regarding

solvation and aggregation but possibly also regarding ligand-bonding modes. For instance, it was recently shown<sup>3</sup> that two closely related sulfur-containing dimeric lithium amide complexes  $[R'(R-S)NLi \cdot xL]_2$  show very different bonding modes around the sulfur atom, monohapto in one case and N–S–Li bridging in the other. These kinds of structural details are of considerable interest because these details have a profound impact on the reactivity (and, more generally, on the properties) of the compounds under investigation.<sup>1,2</sup> On the other hand, they depend quite intricately on subtle details of the system such as the precise nature and concentration of the solvent, L, and of the ligands, R and R'.

Lithium hexamethyldisilazide (LiHMDS) is a prototypical and relatively simple lithium amide complex. As such, it has been studied extensively using a number of experimental techniques.<sup>4–18</sup> Moreover, LiHMDS is a common com-

\* To whom correspondence should be addressed. E-mail: schrecke@cc.umanitoba.ca.

<sup>†</sup> Concordia University.

<sup>‡</sup> University of Manitoba.

<sup>§</sup> Current affiliation: R & D Laboratory, Canadian Technical Tape Ltd., 455 Cote-Vertu Rd., Montreal QC, Canada, H4N 1E8.

<sup>‡</sup> Current affiliation: Department of Chemistry, Lakehead University, 955 Oliver Road, Thunder Bay ON, Canada, P7B 5E1.

(1) Sapse, A.-M.; Schleyer, P. v. R. *Lithium Chemistry: A Theoretical and Experimental Overview*; Wiley: New York, 1995.

(2) Rappoport, Z.; Marek, I. *The Chemistry of Organolithium Compounds*; Wiley: New York, 2004.

(3) Mahmoudkhani, A. H.; Rauscher, S.; Grajales, B.; Vargas-Baca, I. *Inorg. Chem.* **2003**, *42*, 3849.

(4) Kimura, B. Y.; Brown, T. L. *J. Organomet. Chem.* **1971**, *26*, 57.

(5) Williard, P. G.; Liu, Q. Y.; Lochmann, L. *J. Am. Chem. Soc.* **1992**, *114*, 348.

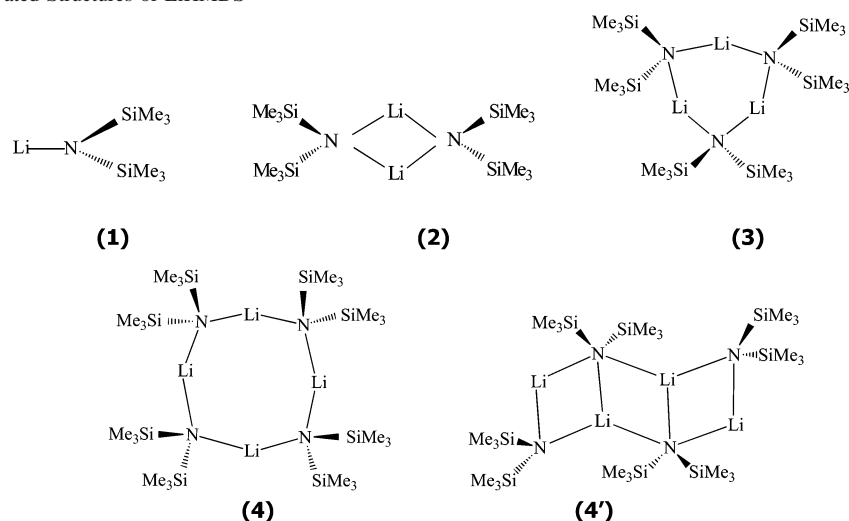
(6) Lucht, B. L.; Collum, D. B. *J. Am. Chem. Soc.* **1994**, *116*, 6009.

(7) Nichols, M. A.; Waldmueller, D.; Williard, P. G. *J. Am. Chem. Soc.* **1994**, *116*, 1153.

(8) Williard, P. G.; Liu, Q.-Y. *J. Org. Chem.* **1994**, *59*, 1596.

(9) Lucht, B. L.; Collum, D. B. *J. Am. Chem. Soc.* **1995**, *117*, 9863.

Scheme 1. Some Unsolvated Structures of LiHMDS



mercially available reagent, and it is widely used in organic synthesis as a strong base and reagent to form other lithium derivatives. LiHMDS can be prepared and used directly in nonpolar solvents or in a mixture of nonpolar and polar solvents. One of the popular mixtures of solvents for LiHMDS is a mixture of pentane (as the nonpolar solvent) with tetrahydrofuran (THF).

Similar to other lithium amides, LiHMDS shows a high propensity in solution, as well as in the solid state, to self-associate into higher aggregates and to form complexes with solvents. The aggregation and solvation degree depends on the choice of solvent and precise conditions.

Theoretical studies on organometallic lithium complexes have been reviewed.<sup>19–21</sup> Previous theoretical studies of lithium amide complexes have usually relied either on small model complexes<sup>22–35</sup> or on using lower-level semiempirical methods such as MNDO, MM3, or PM3. Where ab initio methods have been used on realistic systems, very small (too small) basis sets such as STO-3G have often been used, at the very least for the geometry optimizations.<sup>17,18,22,28,34,36–42</sup>

The goal of the present work is to study the aggregation and microsolvation of LiHMDS using an accurate, modern, standard computational-chemistry method, i.e., density functional theory (DFT<sup>43,44</sup>) utilizing the approximate B3LYP functional,<sup>45–47</sup> and applying it to the *entire* complex without any truncations or model substitutions. Progress in both computer hardware and computational chemistry software has made such an approach possible for the first time.

Specifically, we have studied aggregates from the monomer up to the tetramer ( $n = 1–4$ ), in their unsolvated ( $x = 0$ ) and solvated forms (up to  $x = 4$ ). Some unsolvated and solvated structures are shown schematically in Schemes 1 and 2, respectively.

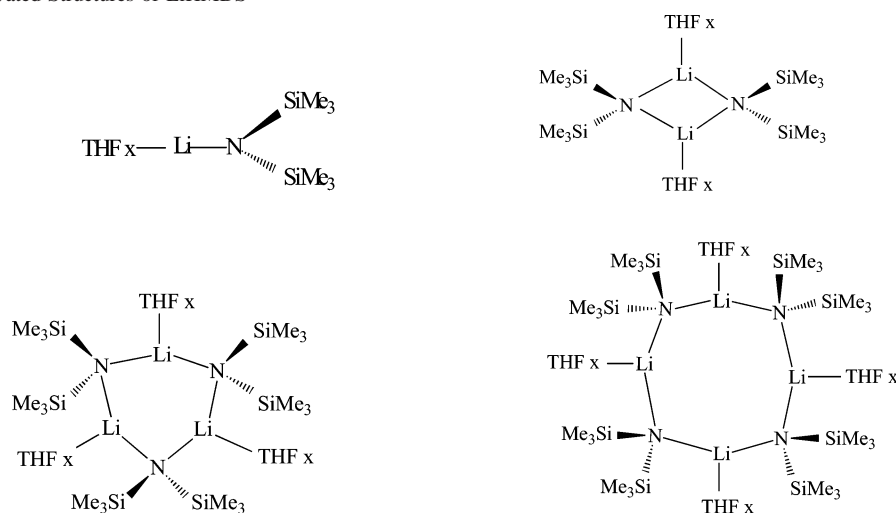
### Computational Methods

All calculations were performed with the Gaussian98 program package.<sup>48</sup> Approximate DFT<sup>43,44</sup> was applied in the form of the hybrid B3LYP exchange-correlation functional.<sup>45–47</sup>

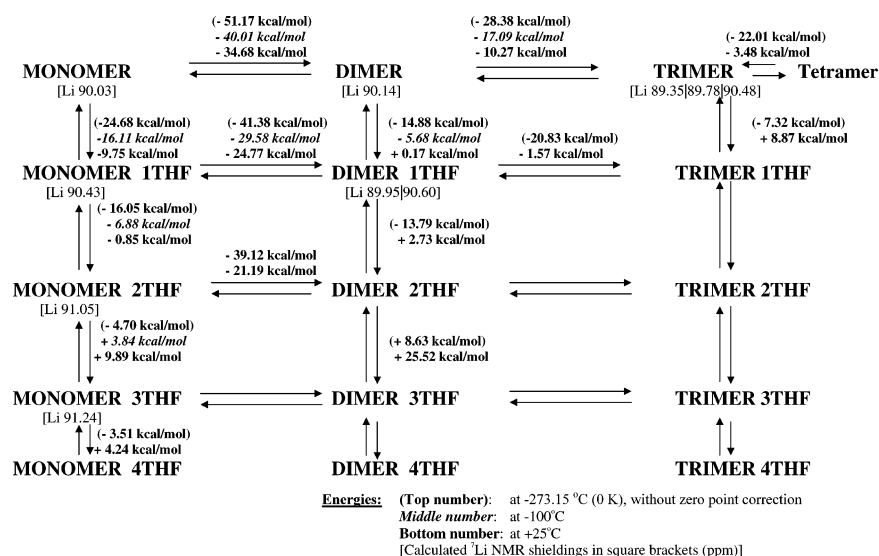
- (10) Lucht, B. L.; Bernstein, M. P.; Remenar, J. F.; Collum, D. B. *J. Am. Chem. Soc.* **1996**, *118*, 10707.
- (11) Lucht, B. L.; Collum, D. B. *J. Am. Chem. Soc.* **1996**, *118*, 2217.
- (12) Lucht, B. L.; Collum, D. B. *J. Am. Chem. Soc.* **1996**, *118*, 3529.
- (13) Lucht, B. L.; Collum, D. B. *Acc. Chem. Res.* **1999**, *32*, 1035.
- (14) Rutherford, J. L.; Collum, D. B. *J. Am. Chem. Soc.* **1999**, *121*, 10198.
- (15) Zhao, P.; Collum, D. B. *J. Am. Chem. Soc.* **2003**, *125*, 4008.
- (16) Fernandez, I.; Martinez-Viviente, E.; Breher, F.; Pregosin, P. S. *Chem. Eur. J.* **2005**, *11*, 1495.
- (17) Romesberg, F. E.; Bernstein, M. P.; Gilchrist, J. H.; Harrison, A. T.; Fuller, D. J.; Collum, D. B. *J. Am. Chem. Soc.* **1993**, *115*, 3475.
- (18) Henderson, K. W.; Dorigo, A. E.; Liu, Q.-Y.; Williard, P. G. *J. Am. Chem. Soc.* **1997**, *119*, 11855.
- (19) Boche, G.; Lohrenz, J. C. W.; Opel, A. In *Lithium Chemistry: A Theoretical and Experimental Overview*; Sapse, A.-M., Schleyer, P. v. R., Eds.; Wiley: New York, 1995; p 195.
- (20) Sapse, A.-M.; Jain, D. C.; Raghavachari, K. In *Lithium Chemistry: A Theoretical and Experimental Overview*; Sapse, A.-M., Schleyer, P. v. R., Eds.; Wiley: New York, 1995; p 45.
- (21) Jemmis, E. D.; Gopakumar, G. In *The Chemistry of Organolithium Compounds*; Rappoport, Z., Marek, I., Eds.; Wiley: New York, 2004; p 1.
- (22) Hilmersson, G.; Arvidsson, P. I.; Davidsson, O.; Haakansson, M. *J. Am. Chem. Soc.* **1998**, *120*, 8143.
- (23) Sapse, A. M.; Kaufmann, E.; Schleyer, P. v. R.; Gleiter, R. *Inorg. Chem.* **1984**, *23*, 1569.

- (24) Kaufmann, E.; Clark, T.; Schleyer, P. v. R. *J. Am. Chem. Soc.* **1984**, *106*, 1856.
- (25) Koch, R.; Anders, E. *J. Org. Chem.* **1994**, *59*, 4529.
- (26) Hoffmann, D.; Dorigo, A.; Schleyer, P. v. R.; Reif, H.; Stalke, D.; Sheldrick, G. M.; Weiss, E.; Geissler, M. *Inorg. Chem.* **1995**, *34*, 262.
- (27) Kremer, T.; Hampel, F.; Knoch, F. A.; Bauer, W.; Schmidt, A.; Gabold, P.; Schütz, M.; Ellermann, J.; Schleyer, P. v. R. *Organometallics* **1996**, *15*, 4776.
- (28) Abboto, A.; Streitwieser, A.; Schleyer, P. v. R. *J. Am. Chem. Soc.* **1997**, *119*, 11255.
- (29) Hilmersson, G. *Chem. Eur. J.* **2000**, *6*, 3069.
- (30) Schulz, H.; Nudelman, N.; Viruela-Martin, P.; Viruela-Martin, R.; Tomas-Vert, F. *J. Chem. Soc., Perkin Trans. 2* **2000**, 1619.
- (31) Fressigné, C.; Maddaluno, J.; Giessner-Prettre, C.; Silvi, B. *J. Org. Chem.* **2001**, *66*, 6373.
- (32) Ganguly, B.; Fuchs, B. *J. Phys. Org. Chem.* **2001**, *14*, 488.
- (33) Pratt, L. M.; Streitwieser, A. *J. Org. Chem.* **2003**, *68*, 2830.
- (34) Ramirez, A.; Lobkovsky, E.; Collum, D. B. *J. Am. Chem. Soc.* **2003**, *125*, 15376.
- (35) Parisel, O.; Fressigne, C.; Maddaluno, J.; Giessner-Prettre, C. *J. Org. Chem.* **2003**, *68*, 1290.
- (36) Bauer, W.; O'Doherty, G. A.; Schleyer, P. v. R.; Paquette, L. A. *J. Am. Chem. Soc.* **1991**, *113*, 7093.
- (37) Romesberg, F. E.; Collum, D. B. *J. Am. Chem. Soc.* **1994**, *116*, 9187.
- (38) Romesberg, F. E.; Collum, D. B. *J. Am. Chem. Soc.* **1995**, *117*, 2166.
- (39) Gaul, C.; Arvidsson, P. I.; Bauer, W.; Gawley, R. E.; Seebach, D. *Chem. Eur. J.* **2001**, *7*, 4117.
- (40) Johansson, A.; Davidsson, O. *Organometallics* **2001**, *20*, 4185.
- (41) Carlier, P. R.; Madura, J. D. *J. Org. Chem.* **2002**, *67*, 3832.
- (42) Yoshida, T.; Sakakibara, K.; Asami, M.; Chen, K.-H.; Lii, J.-H.; Allinger, N. L. *J. Comput. Chem.* **2003**, *24*, 319.

Scheme 2. Some Solvated Structures of LiHMDS



Scheme 3. Computational Aggregation–Solvation Diagram for LiHMDS



We have tested different model chemistries (i.e., combinations of approximate quantum-chemical methods and basis sets) for some small-sized model systems. The combination of B3LYP and the moderate 6-31G(d) basis sets provides the best compromise between

accuracy and computational expediency, as far as structures, vibrational frequencies, and energetics are concerned. This combination of method and basis set amounts to a well-established, standard model chemistry that, even from literature data, should give accurate results for the systems at hand.<sup>44</sup> It has been employed for these properties throughout as a consequence.

All molecules have been optimized without symmetry constraints, unless otherwise noted. Harmonic vibrational frequencies have been calculated in order to verify the nature of each stationary point. These frequencies are also used to calculate thermodynamic properties such as relative free energies. In the (gas-phase) thermochemical analysis, the finite-temperature numbers (Scheme 3, see below) correspond to calculations where all low frequencies that might cause a significant error (as listed in the output) have been removed. (We have not focused on neglecting the vibrations that do not change much during the respective reaction.) Calculations that include all low frequencies into the analysis yield similar numbers.

NMR shieldings and chemical shifts are much more sensitive to the basis sets than, e.g., bond lengths,<sup>44,49</sup> even when an accurate

- (43) Parr, R. G.; Yang, W. *Density-Functional Theory of Atoms and Molecules*; Oxford University Press: New York, Oxford, 1989.
- (44) Koch, W.; Holthausen, M. C. *A Chemist's Guide to Density Functional Theory*; Wiley Verlag Chemie: New York, 2000.
- (45) Becke, A. D. *J. Chem. Phys.* **1993**, *98*, 5648.
- (46) Lee, C.; Yang, W.; Parr, R. G. *Phys. Rev. B* **1988**, *37*, 785.
- (47) Stephens, P. J.; Devlin, F. J.; Chabalowski, C. F.; Frisch, M. J. *J. Phys. Chem.* **1994**, *98*, 11623.
- (48) Frisch, M. J.; Trucks, G. W.; Schlegel, H. B.; Scuseria, G. E.; Robb, M. A.; Cheeseman, J. R.; Zakrzewski, V. G.; Montgomery, J. A., Jr.; Stratmann, R. E.; Burant, J. C.; Dapprich, S.; Millam, J. M.; Daniels, A. D.; Kudin, K. N.; Strain, M. C.; Farkas, O.; Tomasi, J.; Barone, V.; Cossi, M.; Cammi, R.; Mennucci, B.; Pomelli, C.; Adamo, C.; Clifford, S.; Ochterski, J.; Petersson, G. A.; Ayala, P. Y.; Cui, Q.; Morokuma, K.; Malick, D. K.; Rabuck, A. D.; Raghavachari, K.; Foresman, J. B.; Cioslowski, J.; Ortiz, J. V.; Stefanov, B. B.; Liu, G.; Liashenko, A.; Piskorz, P.; Komaromi, I.; Gomperts, R.; Martin, R. L.; Fox, D. J.; Keith, T.; Al-Laham, M. A.; Peng, C. Y.; Nanayakkara, A.; Gonzalez, C.; Challacombe, M.; Gill, P. M. W.; Johnson, B. G.; Chen, W.; Wong, M. W.; Andres, J. L.; Head-Gordon, M.; Replogle, E. S.; Pople, J. A. *Gaussian 98*, revision A.7; Gaussian, Inc.: Pittsburgh, PA, 1998.

- (49) Helgaker, T.; Jaszunski, M.; Ruud, K. *Chem. Rev.* **1999**, *99*, 293.

**Table 1.** Comparison of Selected Calculated Bond Distances (Å) for the Unsolvated and Solvated Monomers [(CH<sub>3</sub>)<sub>3</sub>Si]<sub>2</sub>NLi·xTHF and the Respective Model Compounds [(CH<sub>3</sub>)<sub>2</sub>NLi]<sub>2</sub>·xH<sub>2</sub>O

degree of solvation <i>x</i>	monomer [(CH <sub>3</sub> ) <sub>3</sub> Si] <sub>2</sub> NLi·xTHF			model compound [(CH <sub>3</sub> ) <sub>3</sub> Si] <sub>2</sub> NLi·xH <sub>2</sub> O		
	N–Li	Li–O (THF)	N–Si	N–Li	Li–O (H <sub>2</sub> O)	N–Si
0	1.807		1.708; 1.697			
1	1.829	1.892	1.702; 1.702	1.842	1.915	1.699; 1.698
2	1.891	1.952; 1.952	1.701; 1.701	1.949	1.931; 1.949	1.713; 1.714
3	1.963	2.130; 2.052; 2.046	1.705; 1.704	1.984	2.193; 2.018; 1.935	1.723; 1.723
4	1.974 (1.906) <sup>a</sup>	2.144; 2.057; 2.043; 4.952 (1.955; 1.933; 4.726; 5.458) <sup>a</sup>	1.709; 1.706 (1.700, 1.697) <sup>a</sup>	3.436 <sup>b</sup>	2.054; 2.004; 2.002; 1.857 <sup>b</sup>	1.765; 1.763 <sup>b</sup>

<sup>a</sup> The numbers correspond to structures with 1 and (in parentheses) 2 THF in the second coordination sphere, as is evident from the Li–O distances (see the text). <sup>b</sup> This structure corresponds to  $\{[(\text{CH}_3)_3\text{Si}]_2\text{N}-\text{H}\}^+\{(\text{HO})\text{Li}\cdot 3\text{H}_2\text{O}\}^-$ , see the N–Li distance and the text. The shortest Li–O distance of 1.857 Å corresponds to the OH<sup>−</sup> ligand. The O–H distance for this ligand is 0.966 Å, whereas the O···H(N) distance is 1.708 Å. Note the calculated N–H distance of 1.062 Å.

method such as the GIAO (gauge-including atomic orbitals) approach<sup>50–54</sup> is used. Thus, single-point calculations using the more extensive 6-311+G(d,p) have been used together with the PBE0 hybrid DFT functional<sup>55</sup> to calculate the <sup>6</sup>Li/<sup>7</sup>Li NMR shieldings. This particular model chemistry has been chosen after testing various different combinations of basis set and approximate DFT methods as applied to the <sup>6</sup>Li/<sup>7</sup>Li NMR shieldings (chemical shifts) of a number of small molecules. The DFT-GIAO approach as implemented in Gaussian<sup>54</sup> was employed. The result of theoretical calculations is the absolute shielding. It can be converted to the experimentally observed) chemical shift using the shielding of a suitable reference compound.

## Results and Discussion

**Model Complexes.** Due to the size of the systems and the accompanying computational cost, it is often necessary or at least desirable to choose truncated model complexes. Thus, for LiHMDS, one could replace the bulky –Si(CH<sub>3</sub>)<sub>3</sub> groups by –SiH<sub>3</sub> or methyl groups (or even hydrogens), and the associated THF solvent molecules by the smaller diethylether or water.

We have tested the latter approximation for the LiHMDS monomers using various degrees of solvation with THF and H<sub>2</sub>O, respectively. The results are collected in Table 1. For now, we will concentrate on the differences between the two solvent models. Later, we will also discuss the THF solvation by itself.

The most dramatic effect is seen for the highest degree of solvation, *x* = 4. If the THF solvent is used, then we obtain di- or tri-solvated structures with the remaining two or one THF molecules effectively located in the second coordination sphere (Li–O(THF) distances of about 5 Å), see also below. However, the picture is very different for the H<sub>2</sub>O solvent. Indeed, the water ligand is seen to be a very different ligand than THF in that it breaks the Li–N bond and creates a complex that is best described as consisting of two separate ions,  $\{[(\text{CH}_3)_3\text{Si}]_2\text{N}-\text{H}\}^+$  and  $\{(\text{HO})\text{Li}\cdot 3\text{H}_2\text{O}\}^-$ . This is most

clearly evidenced from the N–Li distance, Table 1, but it follows from an inspection of the calculations (i.e., the O–H and N–H distances, footnote b to Table 1, and the calculated charges) also.

However, even for the lower degrees of solvation where this bond-breaking does not occur (*x* = 1, 2, 3), we see a strong influence of the choice of solvent on the Li–N core of the compounds, as is evident from the respective bond lengths, Table 1. The difference in N–Li bond length amounts to as much as ~0.06 Å for the di-solvated species.

Predictably, the N–Si distances are less influenced by the choice of solvent, Table 1. There is almost no difference between THF and H<sub>2</sub>O solvation for *x* = 1, and that increases to changes of 0.01 and 0.02 Å for *x* = 2 and 3, respectively. The difference is largest for the *x* = 4 case where the geometric and electronic structure is completely altered by the water solvent as compared to the ether, as has been discussed above.

### Structures of the Unsolvated and Solvated Complexes.

Unsolvated and solvated structures are presented schematically in Schemes 1 and 2, respectively. Some of the optimized structures are shown in Figure 1. Selected calculated geometry parameters are provided in Tables 1–3.

A number of interesting trends are apparent upon inspection of the structural data. Let us begin our discussion with the unsolvated species and then extend the analysis to selected solvated ones.

For some of the unsolvated species (Scheme 1), we were able to locate symmetric structures, viz. a structure of *D*<sub>2</sub> symmetry for the dimer **2** and one with (approximate) *D*<sub>4h</sub> symmetry for the ring tetramer **4**, Table 2. We should note that the ladder tetramer **4'** appears to be not stable at this particular level of theory because any attempt at optimizing it resulted in the ring tetramer **4**. The lowest-energy structures for both the monomer **1** and trimer **3** were found to have no symmetry (*C*<sub>1</sub> symmetry only). Finally, we should note that our best tetramer structure **4** still possesses four small imaginary frequencies (between 29i and 11i cm<sup>−1</sup>) that we have been unable to remove, despite several attempts; note also the size of this system and the associated computational cost. Inspection of the output shows that these residual frequencies are related to –CH<sub>3</sub> rotations. In addition, numerical noise might play a role too. In any case, these

(50) London, F. *J. Phys. Radium* **1937**, 8, 397.

(51) Wolinski, K.; Hinton, J. F.; Pulay, P. *J. Am. Chem. Soc.* **1990**, 112, 8251.

(52) Schreckenbach, G.; Ziegler, T. *J. Phys. Chem.* **1995**, 99, 606.

(53) Schreckenbach, G.; Ziegler, T. *Theor. Chem. Acc.* **1998**, 99, 71.

(54) Cheeseman, J. R.; Trucks, G. W.; Keith, T. A.; Frisch, M. J. *J. Chem. Phys.* **1996**, 104, 5497.

(55) Perdew, J. P.; Burke, K.; Ernzerhof, M. *Phys. Rev. Lett.* **1996**, 77, 3865.

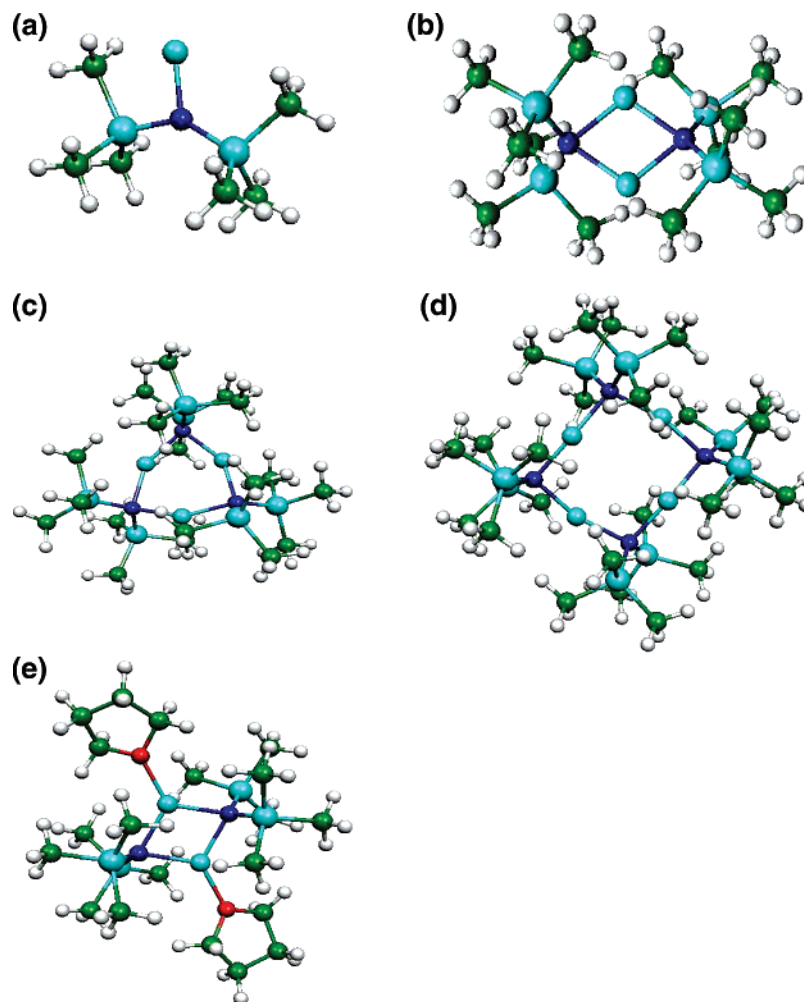


**Figure 1.** B3LYP-optimized structures: (a) unsolvated monomer **1**; (b) unsolvated dimer **2**; (c) unsolvated trimer **3**; (d) unsolvated tetramer **4**; (e) solvated dimer **2**·2THF.

**Table 2.** Selected Bond Lengths (Å) and Angles (deg) for the Unsolvated Aggregated LiHMDS Structures

molecule	symmetry <sup>a</sup>	bond lengths		bond angles	
		Li–N	N–Si	Li–N–Li	N–Li–N
unsolvated monomer <b>1</b>	$C_1$	1.807	1.708; 1.697		
unsolvated dimer <b>2</b>	$D_2$	1.981	1.724	71.0	109.0
unsolvated trimer <b>3</b>	$C_1$	1.987; 1.996; 1.962; 1.991; 2.002; 2.016	1.744; 1.744; 1.743; 1.743; 1.744; 1.745	93.4; 89.8; 88.8	146.0; 146.9; 151.1
unsolvated ring tetramer <b>4</b>	$\sim D_{4h}^b$	1.990; 2.030 <sup>b</sup>	1.755 <sup>b</sup>	101.8 <sup>b</sup>	168.2 <sup>b</sup>

<sup>a</sup> As indicated in the text, the optimizations reported have been performed without symmetry constraint. However, for several cases, we have also attempted to find symmetric structures. The highest (approximate) symmetry corresponding to the global minimum structure is reported here. <sup>b</sup> This structure, though highly symmetric and almost converged with respect to the geometry, still possesses four low-lying imaginary frequencies between 29i and 11i cm<sup>-1</sup> that we have been unable to remove. Note that the ladder tetramer **4'** collapses to the ring tetramer **4**, see the text.

frequencies should thus not have any strong implications on the conclusions of this study.

Increasing the degree of aggregation from the monomer all the way to the tetramer leads to increasing Li–N bond lengths. The largest relative increase appears for the dimer that is the first aggregate, Table 2. The N–Si ligand distances increase as well. The latter point is readily understood from the increasing steric requirements with increasing degree of aggregation. The optimized structures for the different unsolvated aggregates are shown in Figure 1a–d.

Solvated structures have been studied for the monomer, Table 1, and for the aggregates, Table 3. We will begin our discussion with the former. For the monomers, the N–Li bond length is increasing with an increase in the number of THF solvent molecules. On the other hand, the N–Si bond that is situated away from the THF ligands is essentially not affected. While trying to locate a structure with four coordinated THF molecules, we found two minima, none of which corresponds to a true tetra-solvated species, Table 1. Instead, we find either a tri-solvated species with one THF

**Table 3.** Bond Lengths (Å) and Angles (deg) for Selected Solvated Aggregated LiHMDS Structures

molecule	bond lengths			bond angles	
	Li–N	N–Si	Li–O	Li–N–Li	N–Li–N
monosolvated dimer <b>2</b> ·1THF	1.962; 2.059	1.730; 1.728	1.951	71.6; 71.6	104.6; 112.3
disolvated dimer <b>2</b> ·2THF <sup>a</sup>	2.032; 2.035; 2.037; 2.041	1.730; 1.728; 1.730; 1.730	1.970; 1.972	73.0; 73.0	107.0; 106.7
trisolvated “open dimer” <b>2</b> ·3THF	2.083; 2.029; 1.900 (4.605)	1.741; 1.742; 1.717; 1.712	2.065; 2.232; 2.066	98.4	173.3
monosolvated trimer <b>3</b> ·THF	1.975; 1.982; 1.986; 1.975; 2.158; 2.160	1.749; 1.748; 1.749; 1.748; 1.755; 1.754	2.052	95.8; 96.5; 87.2	154.6; 153.8; 132.0

<sup>a</sup> Dimer with one THF ligand per Li  $\{[(\text{CH}_3)_3\text{Si}]_2\text{NLi}\cdot\text{THF}\}_2$ , see the text.

in the second solvation sphere, as indicated by the Li–O(THF) bond length of 4.952 Å, or a di-solvated molecule with two THF in the second coordination sphere (Li–O(THF) bond length of 4.726 and 5.458 Å, respectively; data in parentheses in Table 1). Thus, we conclude that the highest possible degree of solvation for the monomer is three, see also below.

Geometry parameters for selected solvated aggregated structures are collected in Table 3.

Adding one THF molecule to the dimer, **2**·1THF, leads to lengthened Li–N bond lengths of 2.059 Å on the solvated side and shortened Li–N bond lengths on the opposite side of the  $\text{Li}_2\text{N}_2$  ring, as compared to the unsolvated dimer that has a bond length of 1.981 Å. (The smaller N–Li–N angle of 104.6° corresponds to the solvated side of the ring, accordingly. The THF molecule is slightly rotated, leading to an overall structure without symmetry.) The bond lengths effects should be due to both steric and electronic factors.

Attempts to locate a structure where the THF solvent is bridging the ring by bonding to both Li atoms lead to either a transition state structure with one imaginary frequency of 126i  $\text{cm}^{-1}$ , or back to the structure with the solvent coordinating one Li atom only. We conclude that the bridged mono-solvated structure likely does not exist.

Excluding bridged structures which is reasonable from the preceding discussion, there are two possible structures for the di-solvated dimer **2**·2THF, one with both THF molecules coordinating to the same side of the  $\text{Li}_2\text{N}_2$  ring, i.e., to the same Li atom, and another that has one solvent (THF) molecule per Li atom. The latter has been included in Table 3 and is shown in Figure 1e; we did not include a structure for the former isomer that is expected to be significantly higher in energy due to steric factors. Similar to the case of the monomer and mono-solvated dimer, THF solvation leads to a lengthening of the Li–N bonds but leaves the N–Si bonds essentially unaffected (only a very slight increase in bond lengths of 0.004–0.006 Å), Table 3.

Similar to the di-solvated dimer, there are again two possible structures for the tri-solvated dimer **2**·3THF, one with all three THF molecules coordinating to the same side of the  $\text{Li}_2\text{N}_2$  ring, i.e., to the same Li atom, and the other having one or two solvent (THF) molecules per Li atom, respectively. The latter isomer is again, of course, the most stable one due to steric factors. This time, however, we would like to briefly discuss the former isomer also as attempts at optimizing it lead to the “open dimer” structure. (This can

be related to the fact that five-coordination on Li is unrealistic; the “open dimer” has a four-coordinated solvated Li.) This “open dimer” structure has also been included into Table 3 where the Li–N bonds are listed in order starting from the solvated Li toward the terminal nitrogen. Thus, the shortest bond length of 1.900 Å corresponds to the terminal nitrogen. We provide the nonbonded distance between the terminal N and Li atoms in brackets. Note the sterically induced lengthening of the Li–O(THF) bonds.

For the trimer, we have only studied the mono-solvated species **3**·1THF, Table 3, since already this species is energetically unfavorable as compared to the unsolvated one (see below). The longer Li–N bond lengths correspond again to the solvated side of the ring, as does the smallest N–Li–N angle.

**<sup>6</sup>Li/<sup>7</sup>Li NMR Shieldings.** NMR methods are used extensively for the experimental study of the solution structure, energetics, and equilibria of lithium amides (e.g., refs 7, 12, 14, 15, 17, 29, 56–64 see also various reviews<sup>65–69</sup>), and much of the information regarding likely solution species or equilibria has been obtained from this technique. Not always is the assignment unequivocal, though, especially in high-symmetry cases, which can lead to experimental information on lithium amide structures that is contradictory. Thus, it would be useful to relate the observed NMR

- (56) Bernstein, M. P.; Romesberg, F. E.; Fuller, D. J.; Harrison, A. T.; Collum, D. B.; Liu, Q. Y.; Williard, P. G. *J. Am. Chem. Soc.* **1992**, *114*, 5100.
- (57) Gilchrist, J. H.; Collum, D. B. *J. Am. Chem. Soc.* **1992**, *114*, 794.
- (58) Gemünd, B.; Nöth, H.; Sachdev, H.; Schmidt, M. *Chem. Ber.* **1996**, *129*, 1335.
- (59) Aubrecht, K. B.; Lucht, B. L.; Collum, D. B. *Organometallics* **1999**, *18*, 2981.
- (60) Armstrong, D. R.; Henderson, K. W.; Kennedy, A. R.; Kerr, W. J.; Mair, F. S.; Moir, J. H.; Moran, P. H.; Snaith, R. *J. Chem. Soc. Dalton Trans.* **1999**, 4063.
- (61) Andrews, P. C.; Duggan, P. J.; Fallon, G. D.; McCarthy, T. D.; Peatt, A. C. *J. Chem. Soc. Dalton Trans.* **2000**, 1937.
- (62) Amedjkouh, M.; Pettersen, D.; Lill, S. O. N.; Davidsson, O.; Ahlberg, P. *Chem. Eur. J.* **2001**, *7*, 4368.
- (63) Chivers, T.; Krahn, M.; Parvez, M.; Schatte, G. *J. Chem. Soc. Chem. Commun.* **2001**, 1922.
- (64) Al-Masri, H. T.; Sieler, J.; Hey-Hawkins, E. *Appl. Organomet. Chem.* **2003**, *17*, 641.
- (65) Collum, D. B. *Acc. Chem. Res.* **1993**, *26*, 227.
- (66) Hartung, M.; Günther, H.; Amoureux, J.-P.; Fernandez, C. *Magn. Reson. Chem.* **1998**, *36*, S61.
- (67) Boman, A.; Johnels, D. *Magn. Reson. Chem.* **2000**, *38*, 853.
- (68) Zabicky, J. In *The Chemistry of Organolithium Compounds*; Rappoport, Z., Marek, I., Eds.; Wiley: New York, 2004.
- (69) Johnels, D.; Günther, H. In *The Chemistry of Organolithium Compounds*; Rappoport, Z., Marek, I., Eds.; Wiley: New York, 2004; p 137.

**Table 4.** MNDO Reaction Enthalpies According to Romesberg et al.<sup>17</sup> (kcal/mol)

reactant	product	MNDO enthalpy <sup>a</sup>
monomer <b>1</b>	dimer <b>2</b>	-23.8
dimer <b>2</b>	trimer <b>3</b>	+4.6
dimer <b>2</b>	tetramer <b>4</b>	+8.5
monomer·2THF ( <b>1</b> ·2THF)	dimer·2THF ( <b>2</b> ·2THF)	-1.7

<sup>a</sup> Reference 17.

parameters to the calculated ones and, in this way, to the electronic structure and the geometry. As a first step in this direction, we have calculated the isotropic <sup>6</sup>Li/<sup>7</sup>Li NMR absolute shieldings. Results are presented in Scheme 3 (numbers in square brackets) where we also summarize the energetics of aggregation and solvation, to be discussed below.

We have chosen absolute shieldings,  $\sigma$ , over chemical shifts,  $\delta$ , because of the difficulty in modeling the experimental standard (reference compound), usually aqueous solutions of LiCl or LiBr. Shieldings and shifts are related by

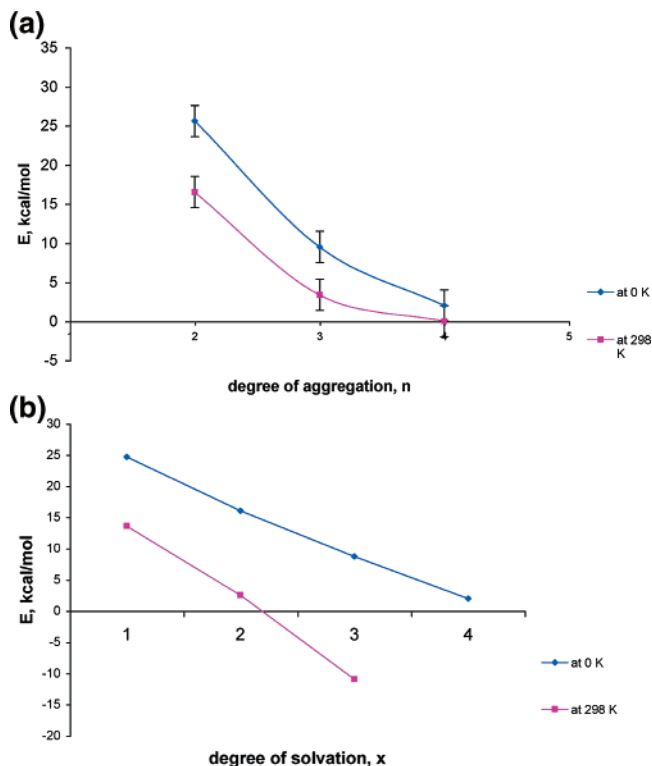
$$\delta = \sigma_{\text{ref}} - \sigma \quad (1)$$

where  $\sigma_{\text{ref}}$  is the isotropic shielding of the reference compound. If the chemical shift is required, it would be preferable to use an “internal standard” such as the most stable compound in a given group. In any case, we note that differences in shieldings and chemical shifts have opposite signs, eq 1.

Analyzing the NMR data in Scheme 3, we note a distinct, monotonic increase in shielding (decrease in chemical shift) upon successive addition of THF solvent molecules. The increase amounts to 0.4, 0.6, and 0.2 ppm, for the formation of mono-, di-, and trisolvated monomers, respectively.

The situation is less clear-cut for the dimer and trimer because they contain potentially inequivalent lithium sites, and moreover, some kind of dynamic average is observed in solution. Overall, there is no clear relationship between structure and lithium shielding (chemical shift) for these species.

For some of the complexes, we have also analyzed the calculated shielding in terms of the electronic structure, viz. the molecular orbitals (MOs). This MO analysis has, at times, been extremely powerful in explaining trends in chemical shifts across series of related compounds (e.g., refs 70–73). In these cases, it was always one or, at most, a few pairs of occupied and virtual MOs coupled by the magnetic field that determined the trends entirely. However, for all LiHMDS complexes analyzed, we find always a large number of relatively small contributions that contribute with approximately equal weights, and no trends could be found.

(70) Ruiz-Morales, Y.; Schreckenbach, G.; Ziegler, T. *J. Phys. Chem.* **1996**, *100*, 3359.(71) Ruiz-Morales, Y.; Schreckenbach, G.; Ziegler, T. *Organometallics* **1996**, *15*, 3920.(72) Schreckenbach, G. *J. Chem. Phys.* **1999**, *110*, 11936.(73) Schreckenbach, G. *Inorg. Chem.* **2002**, *41*, 6560.

**Figure 2.** Stabilization energy per Li atom vs (a) degree of aggregation  $n$  for unsolvated LiHMDS oligomers and (b) degree of solvation,  $x$ ; 0 K (diamonds, top line) and 298 K (squares, bottom line), respectively.

**Energetics.** A computational aggregation–solvation diagram for LiHMDS is shown in Scheme 3. For the different equilibria of aggregation or solvation, we provide the free energy at 0 K (number in brackets), and the free energy at  $-100$  °C (number in *italic*, where available), and the free energy at 298.15 K, 25.0 °C (provided as the bottom number). In each case, a negative free energy means that the product is more favorable than the reactant. (In the following discussion, we consider as the product the species on the right-hand side of a horizontal reaction or on the bottom of a vertical reaction.) We also show the calculated <sup>6</sup>Li/<sup>7</sup>Li NMR shieldings (in brackets) that have been discussed separately above.

Romesberg et al.<sup>17</sup> have studied some of the same equilibria using semiempirical MNDO calculations. Calculated reaction enthalpies,  $\Delta H$ , from this work are provided in Table 4. These MNDO numbers can be compared to our  $\Delta G$  values as provided in Scheme 3.

Let us start with the successive aggregation processes by considering the unsolvated species only. An analysis of the DFT-calculated free energies for the unsolvated LiHMDS oligomers, presented in the top line of Scheme 3, shows that, the higher the degree of aggregation,  $n$ , the more stable the structure. However, the gain of energy per Li atom with increase of  $n$  is not linear but rather inverse exponential. Figure 2a shows the gain of stabilization energy at two different temperatures versus the degree of aggregation. From this figure, one can see that, for degrees of aggregation greater than four, the gain in energy is negligible and amounts to less than 0.5 kcal/mol per monomeric unit at 0 K (without zero-point correction to the energy). It is even smaller at

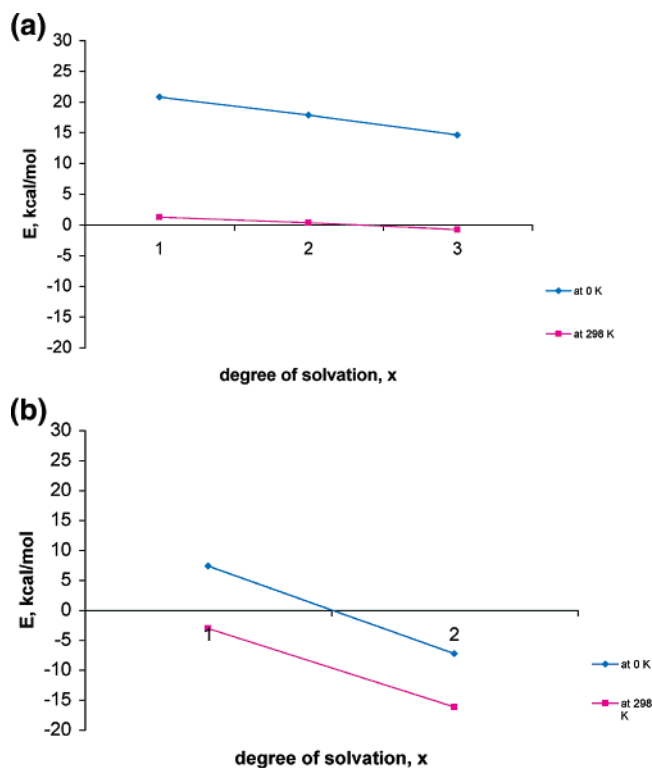


**Figure 3.** Stabilization energy per molecule of (a) dimer and (b) trimer vs degree of solvation; 0 K (diamonds, top line) and 298 K (squares, bottom line), respectively.

higher temperatures. In solution, where there is an interaction between solvent molecules and LiHMDS, and in the solid state, where the interactions between different LiHMDS molecules are even more significant, the degree of aggregation might be similar or less. Therefore, the most probable highest degree of aggregation at 298 K will not exceed  $n = 4$ . This is consistent with the largest observed LiHMDS oligomer in pentane solution being the cyclic tetramer, and in the solid state, the trimer.

The preceding conclusions are not borne out by the MNDO calculations of Romesberg et al.,<sup>17</sup> Table 4, who find positive  $\Delta H$  values already for the dimer–trimer equilibrium. MNDO thus predicts lower degrees of aggregation than DFT.

For the solvated monomer, differences in energy show that addition of the next THF molecule increases the stability at 0 K until the solvent coordination number reaches  $x = 3$ , for a total coordination number of four at the lithium atom. After that, the addition of THF becomes unfavorable, Figure 2b. This has been discussed before from the point of view of the geometries, and it should be due to steric factors. Similar trends are seen for the solvated dimeric and trimeric LiHMDS, Figure 3a and b. Addition of each subsequent THF molecule to the LiHMDS aggregates produces a lesser stabilization effect than the addition of the previous one. This is especially true for the higher degrees of aggregation, Figure 3a and b.

In addition to the curves for 0 K, Figures 2b and 3 also show the gain in energy per molecule of LiHMDS versus degree of solvation at 298 K. For the monomer at this temperature, addition of the first and the second THF molecule is favorable, as it leads to more stable species. The

dimer shows similar trends. For the trimer, though, even the addition of just one THF molecule is now unfavorable. Overall, we conclude from Figures 2b and 3 that the higher the degree of aggregation  $n$ , the fewer THF molecule can complex Li. Moreover, all of this is in good agreement with experimental data for THF solution, where the di-solvated dimer and monomer are observed.<sup>6,9,10</sup> It is also consistent with the existence of the di-solvated dimer in the solid phase.<sup>18</sup>

Calculated differences in (gas-phase) energies can be used to predict which species are thermodynamically more stable at the given level of theory. Assuming full transferability from gas-phase calculations to solution, these results can then be used to—cautiously—make predictions as to which species might exist in THF or pentane solutions after reaching equilibrium. For example, from one of the possible chains of reactions, an analysis of  $\Delta G$  for the transformation:



(the decomposition of the solvated trimer) shows that the reaction is much more favorable as written at 298 K ( $\Delta G = -11.0$  kcal/mol) than at 0 K ( $\Delta G = 7.6$  kcal/mol). It also explains why no trimer exists in THF solutions of high concentration and experimental temperatures, where only the solvated dimer and monomer are observed.<sup>6,9,10</sup> A further analysis shows that the mono-solvated monomer and unsolvated dimer (i.e., the products of reaction 2) readily attach additional THF molecules, up to a coordination number of four at the lithium. This leads to further stabilization, as discussed in detail above (Figures 2b and 3a), further driving reaction 2 to the right-hand side. The overall process is again temperature-dependent such that at very low temperatures (close to 0 K), the deaggregation reaction 2 does not take place, but at higher temperatures (298 K) only the smaller species with higher degrees of solvation are stable (with a solvent coordination number of  $x = 2$  or 3 for the monomer and  $x = 2$  for the dimer, Figures 2b and 3a).

In a similar fashion, one can predict that, at 298 K, the tri-solvated dimer gives rise to a di-solvated monomer and a mono-solvated dimer. Solvated monomers and dimers are the most stable solvated species in the system.

Finally, let us consider nonpolar solvents, i.e., solutions where no THF is present. The unsolvated monomer at 298 K is not observed experimentally. This is consistent with the high energy requirement for its formation according to the following reaction (Scheme 3):



A possible path for dimer formation from the trimer (which is the preferred oligomer in the solid state), in the absence of THF, involves the following two reactions:



for a net reaction as follows





In other words, the trimer–dimer equilibrium (in the absence of THF or other polar solvents) probably involves a bimolecular mechanism with an intermediate tetramer.

## Conclusions

In this paper we have presented a detailed computational study of LiHMDS species in various degrees of aggregation and microsolvation. To the best of our knowledge, this is the first such study that applies reliable modern DFT to the complete complexes without truncation of the bulky ligands. We have shown the importance of using a modern quantum-chemical method, as the results differ qualitatively between our B3LYP calculations and older semiempirical MNDO calculations from the literature.<sup>17</sup> We have likewise shown (by way of example) the dangers inherent in using truncated model ligands instead of the real, experimentally observed systems, Table 1. The computational hardware and software have reached a point that this can actually be done for the first time.

We have reported calculated  $^6\text{Li}/^7\text{Li}$  NMR absolute shieldings for a number of species, Scheme 3. While some trends are apparent from the calculations (notably an increase in shielding—decrease in chemical shift—upon successive solvent coordination), in general, calculated lithium shieldings (chemical shifts) alone seem to be insufficient for unequivocal assignments of the different species. This is principally due to difficulties in modeling dynamic effects. We should also keep in mind that any bulk effects of the solvent have been neglected in our calculations. As for converting absolute shieldings into chemical shifts (eq 1), it appears preferable to use some internal standard instead of the—difficult to model—experimental one. We conclude that future studies should attempt to also calculate and interpret a wider range of NMR observables, including the chemical shift tensor, quadrupolar couplings, NMR of other nuclei, or spin–spin couplings.

The study of the energetics of aggregation and solvation has been the central focus of this article, Scheme 3. Here, we have seen the importance of including entropy corrections

(to give free energies) and temperature effects: The degrees of both solvation and aggregation are generally higher at 0 K than at 298 K. Another important result is that the current DFT calculations yield a qualitatively different picture than the older (semiempirical) MNDO calculations of Romesberg et al.,<sup>17</sup> Table 4 and Scheme 3. MNDO predicts the trimer and tetramer formation to be energetically unfavorable, whereas we find that the highest possible degree of aggregation for unsolvated LiHMDS is four.

The energy gain per monomer unit is seen to be decreasing with increasing degrees of aggregation, Figure 2a, leading to the mentioned maximum degree of aggregation of four. This energy gain is also temperature dependent. The stabilization energy of solvation is likewise a function of both the number of solvent (THF) molecules and of temperature, Figures 2b and 3.

While the highest possible degree of aggregation was found to be four, the picture is different for solvation in nonpolar solvents, where we have shown that the formation of the LiHMDS dimer (from the solid trimers) is preferred over alternative species, reactions 4–6. The pathway is likely to involve an intermediate tetramer, reactions 4 and 5. A monomer, however, is not expected to exist, cf. reaction 3.

If, however, a polar solvent such as THF is present, then both the monomer and the dimer are formed (reaction 2). Thus, given the most probable degree of solvation for these species at 298 K being two (Figures 2b and 3a), di-solvated monomers and dimers are the most likely species in THF solution.

**Acknowledgment.** Financial support from the Natural Sciences and Engineering Research Council of Canada (NSERC) and the Fonds de Recherche sur la Nature et les Technologies du Québec (NATEQ) is acknowledged. G.S. is grateful to I. Vargas-Baca, McMaster University, for suggesting the project and for helpful discussions. G.S. further acknowledges the work of A. Carrasco who contributed to the project.

IC061599S